Manuscript prepared for Atmos. Chem. Phys.
with version 3.0 of the LaTeX class copernicus.cls.
Date: 16 May 2012

Supplement for "Aerosol- and greenhouse gas-induced changes in summer rainfall and circulation in the Australasian region: a study using single-forcing climate simulations"

L. D. Rotstayn[1], S. J. Jeffrey[2], M. A. Collier[1], S. M. Dravitzki[1], A. C. Hirst[1], J. I. Syktus[2], and K. K. Wong[2]

[1]Centre for Australian Weather and Climate Research, CSIRO Marine and Atmospheric Research, Aspendale, Vic, Australia
[2]Queensland Climate Change Centre of Excellence, Dutton Park, Qld, Australia

Abstract. Supplementary material consists of (1) a description of the CSIRO-Mk3.6 GCM, with a primary focus on the aspects that differ from earlier versions, (2) an overview of the global-mean aerosol simulation, (3) breakdown of anthropogenic aerosol forcing into direct and indirect effects.

S1 Model description

S1.1 Overview

The CSIRO Mark 3.6 (CSIRO-Mk3.6) GCM was developed from the earlier Mk3.5 version, which was described in detail by Gordon et al. (2002, 2010). It is a coupled atmosphere-ocean model with dynamic sea ice. It also has a soil-canopy scheme with prescribed vegetation properties. The ocean, sea-ice and soil-canopy models are unchanged between Mk3.5 and Mk3.6. The main differences between Mk3.5 and Mk3.6 are the inclusion of an interactive aerosol treatment and an updated radiation scheme in Mk3.6. Rotstayn et al. (2010) gave an overview of CSIRO-Mk3.6; they also assessed the model's simulation of Australian mean climate and natural rainfall variability associated with ENSO, with generally favourable conclusions. Here, we briefly describe the main components of the model, with more detail about the aerosol and radiation treatments in Sect. S1.2.

The atmospheric component is a spectral model, which utilizes the flux form of the dynamical equations (Gordon, 1981). It has 18 vertical levels and horizontal resolution of approximately $1.875^\circ \times 1.875^\circ$ (spectral T63). Advection of water vapour, cloud water and trace quantities is not treated spectrally; vertical advection is handled using a flux-corrected transport scheme (Van Leer, 1977), and horizontal advection is handled using a semi-Lagrangian scheme (McGregor, 1993).

Correspondence to: L. D. Rotstayn (leon.rotstayn@csiro.au)

The main aspects of the atmospheric physics package (other than radiation and aerosols) are as follows. Convection is treated using the mass-flux scheme of Gregory and Rowntree (1990), modified by the inclusion of downdrafts (Gregory, 1995). The treatment of surface fluxes and vertical turbulent mixing is based on stability-dependent K-theory (Louis, 1979). Under convective conditions, an additional non-local counter-gradient flux is added in the boundary layer (Holtslag and Boville, 1993); this feature was not included in Mk3.5. The stratiform cloud and precipitation scheme was described by Rotstayn (1997, 1998), with an improved treatment of mixed-phase clouds as in Rotstayn et al. (2000). The scheme includes a simple parameterization of fractional cloudiness, prognostic variables for cloud liquid water and cloud ice, and physically distinct treatments of warm-rain and frozen-precipitation processes. Interactions between the cloud and aerosol schemes are described in Sect. S1.2.

The ocean model is based on version 2.2 of the Modular Ocean Model (MOM2.2; Pacanowski, 1996). Every atmospheric grid-box is coupled to two oceanic grid-boxes: enhanced north-south resolution in the ocean model was implemented with the aim of improving the representation of tropical variability. The ocean model thus has resolution of approximately $0.9375^\circ \times 1.875^\circ$ and has 31 vertical levels. Several improved physical parameterizations were implemented in Mk3.5 to reduce biases and climate drift in the earlier Mk3.0 version (Gordon et al., 2002, Fig. 22). In particular, the ocean model was upgraded to include spatially varying eddy-transfer coefficients (Visbeck et al., 1997) and a revised parameterization of mixed-layer depth (Kraus and Turner, 1967). Changes to the ocean-atmosphere coupling included an improved river-routing scheme, with time-delay due to flow (Gordon et al., 2010). The sea-ice model is based on O'Farrell (1998), with revised numerics as described by Gordon et al. (2010).

S1.2 Interactive aerosol scheme

There are 11 prognostic mass tracers in the aerosol scheme: dimethyl sulfide (DMS), sulfur dioxide (SO_2), sulfate, hydrophobic and hydrophilic forms of black carbon (BC) and organic carbon, and four size bins of mineral dust, with radii ranging from 0.1–1, 1–2, 2–3 and 3–6 μm respectively. A factor of 1.3 is used to convert the mass of organic carbon to the mass of organic aerosol (OA) (Penner et al., 1998). Number concentrations of two modes of sea salt (film-drop and jet-drop) are diagnosed as a function of 10-m wind speed in the marine boundary layer (O'Dowd et al., 1997), but are not treated prognostically.

Prescribed anthropogenic and biomass-burning sources of sulfur, BC and OA are based on the recommended data sets for CMIP5 (Lamarque et al., 2010), with some modifications. We uniformly increased the emissions of BC (by 25 %) and OA (by 50 %) to improve the agreement between modelled and observed fields of carbonaceous aerosol. Similar adjustments were applied in earlier versions of the model (Rotstayn et al., 2007, 2010). We justified this by the large uncertainty in emissions of carbonaceous aerosol (Bond et al., 2004), and the standard inventory's omission of anthropogenic secondary organic aerosol (SOA), which can substantially enhance effective emissions of OA (Kanakidou et al., 2005; Lee et al., 2008). The relatively small emissions of black carbon from aviation were omitted from our simulations. With these adjustments, the annual emission of BC in the year 2000 is 9.7 Tg (compared to 7.7 Tg in the standard inventory), and the emission of OA from anthropogenic and biomass-burning sources is 53 Tg C (compared to 35 Tg C in the standard inventory).

Prescribed natural sources of sulfur comprise SO_2 from continuously erupting volcanoes (8.0 Tg S yr^{-1}) and biogenic emissions of DMS from oceans, soils and plants (0.9 Tg S yr^{-1}) (Rotstayn and Lohmann, 2002). The oceanic DMS source is calculated from a global database of DMS measurements, and is thus representative of modern-day climate (Kettle et al., 1999; Kettle and Andreae, 2000). The DMS flux parameterization is based on the quadratic relation from Nightingale et al. (2000) for wind speeds below 13 m s^{-1} and the piecewise-linear relation from Liss and Merlivat (1986) for wind speeds above 18 m s^{-1}, with a linear transition between them at wind speeds from 13 to 18 m s^{-1}. A parameterization of sub-grid gustiness due to deep convection and free convection is included, analogous to that used in the dust scheme (Rotstayn et al., 2011). With these treatments, the global oceanic DMS source is 27 Tg S yr^{-1} in 2000, which is larger than the source of 18 Tg S yr^{-1} prescribed for the AeroCom models (Dentener et al., 2006). However, an updated DMS database (Lana et al., 2011) indicates that global DMS emissions are larger than previously thought, with a best estimate of 28.1 Tg S yr^{-1}, so the emissions in our model may not be excessive.

The prescribed climatological source of natural SOA assumes rapid conversion to OA of a fixed percentage of the terpene emission from Guenther et al. (1995); earlier versions of the model assumed a yield of 13 %, giving a global source of 16.4 Tg C per annum. In view of evidence that this may seriously underestimate global production of biogenic SOA (Kanakidou et al., 2005; Goldstein and Galbally, 2007), the yield was increased to 28 %, corresponding to a global source of 35 Tg C. However, recent work by Pye et al. (2010) suggests that this may be an overestimate: using a global chemical transport model, they estimated that 14–15 Tg yr^{-1} of SOA is formed from terpenes and 8–9 Tg yr^{-1} from isoprene, for a total yield of 22–24 Tg yr^{-1} of biogenic SOA.

The treatment of mineral dust emission follows Ginoux et al. (2001, 2004). The scheme is based on satellite retrievals from the Total Ozone Monitoring Spectrometer (TOMS), which indicate that most large dust sources correspond to topographic depressions (Prospero et al., 2002). Further details of the dust scheme are given by Rotstayn et al. (2011), who obtained global dust emissions of 3569 Tg for the year 2000. This is somewhat larger than the range of 1000 to 3000 Tg yr^{-1} that was found to be consistent with observations by Cakmur et al. (2006). Rotstayn et al. (2011) attributed the relatively large dust emission to the model's implementation of a sub-grid gustiness parameterization, and noted that this was the likely cause of a global dust burden close to the high end of the range found in other dust models.

Treatments of aerosol transformations are limited to oxidation reactions involving sulfate precursors, and a simple time-dependent decay of hydrophobic carbonaceous aerosols to their respective hydrophilic forms. The treatment of tropospheric sulfur chemistry is based on Feichter et al. (1996), with modifications as in Rotstayn and Lohmann (2002). The carbonaceous aerosol module (Cooke et al., 1999) assumes a fixed e-folding time of 1 day for the conversion of BC and OA from their hydrophobic to hydrophilic forms.

Tracer transport occurs by advection, vertical turbulent mixing and vertical transport inside deep convective clouds. The treatments of advection and vertical turbulent mixing were described in Sect. S1.1. Convective tracer transport is based on the vertical profiles of the updraft mass flux and compensating subsidence generated by the convection scheme (Gregory and Rowntree, 1990); further details are given by Rotstayn and Lohmann (2002).

Prognostic aerosols are removed from the atmosphere by wet and dry deposition, and (for dust) by gravitational settling. Wet deposition processes include in-cloud and below-cloud scavenging by rain and snow (Rotstayn and Lohmann, 2002). Dry deposition processes follow Lohmann et al. (1999) for sulfate, SO_2 and carbonaceous aerosol. The treatments of dry deposition and gravitational settling of dust follow Ginoux et al. (2001).

S1.3 Radiation and indirect aerosol effects

The aerosol treatments in CSIRO-Mk3.6 are supported by an updated radiation scheme that can treat aerosol-radiative effects (which was not possible in Mk3.5). The radiation scheme includes the shortwave effects of all the above aerosol types and the longwave effects of dust and stratospheric aerosol. Details of the aerosol optical properties, including the treatment of hygroscopic growth, are given by Rotstayn et al. (2007), with updates to the dust treatment described by Rotstayn et al. (2011). The shortwave radiation scheme is a two-stream code with 12 bands and 24 k terms (Grant and Grossman, 1998; Grant et al., 1999). The longwave scheme has 10 bands – a combination of k distribution and pre-computed transmittances (Grant et al., 1999; Chou and Lee, 2005). Another advantage of the new radiation scheme is the ability to treat non-CO_2 GHGs (methane, nitrous oxide and halocarbons), avoiding the need for the "equivalent CO_2" approximation that was used in Mk3.5.

The model also includes treatments of aerosol indirect effects on liquid-water clouds. The parameterisation of cloud droplet number concentration ($N_{\rm d}$, in $\rm m^{-3}$) is based on the relation from Jones et al. (1994), namely

$$N_{\rm d} = \max\{375 \times 10^6 (1 - e^{-2.5\times10^{-9}A}), N_{\rm min}\}, \qquad (1)$$

where $N_{\rm min} = 10 \times 10^6$ and A is the number concentration of hydrophilic aerosols (in $\rm m^{-3}$). In the radiation scheme, carbonaceous aerosols (OA and BC) are assumed to exist as an internal mixture, and all other aerosol species are externally mixed; for consistency, this assumption is also applied to the calculation of $N_{\rm d}$. Thus A is taken as the sum of the concentrations of sulfate, sea salt and hydrophilic carbonaceous aerosol. The conversion from aerosol mass concentration $m_{\rm s}$ (carried prognostically by the model) to aerosol number $A_{\rm s}$ for sulfate and carbonaceous aerosol is based on the same (prescribed) mass-number relationship that is used for that species in the radiation scheme. Thus if $m_{\rm s}$ and $m_{\rm c}$ are respectively the mass concentrations of sulfate and hydrophilic carbonaceous aerosol (OA plus BC) in $\rm kg\,m^{-3}$, $A = 5.1 \times 10^{17} m_{\rm s} + 3.0 \times 10^{17} m_{\rm c}$. The windspeed-dependent diagnostic relation for sea salt in the marine boundary layer provides number concentrations of sea salt (O'Dowd et al., 1997), so no conversion is necessary. Note that the use of Eqn. (1) entails the simplifying assumption that the different aerosol species have the same efficiency as CCN, whereas in reality carbonaceous aerosol is less soluble than sulfate and sea salt.

Equation (1) feeds into the calculation of cloud droplet effective radius, which includes a parameterization of the observed increase of droplet spectral dispersion with increasing $N_{\rm d}$ (Rotstayn and Liu, 2009). In stratiform clouds, Eq. (1) also feeds into the calculation of drizzle formation ("autoconversion"; Rotstayn and Liu, 2005), which affects the persistence of liquid water clouds (the so-called second indirect effect). The autoconversion scheme also includes a simple parameterization of sub-grid cloud-water variability, whereby only the part of the grid box in which the cloud liquid-water content exceeds the autoconversion threshold is used in the calculation of autoconversion (Rotstayn, 2000); one effect of this parameterization is to reduce the magnitude of the simulated second indirect effect, for a given treatment of the autoconversion rate and threshold.

The aerosol treatments in our model are simplified in many respects. For example, a limitation of the single-moment scheme is that different aerosol modes cannot interact (e.g. by coagulation or heterogeneous chemistry). Parameterization of cloud droplet number concentration as an empirical function of aerosol number ignores much of the subtle physics and chemistry of cloud droplet nucleation. These and other limitations are discussed in more detail by Rotstayn et al. (2007). Having said that, similar simplifications are adopted in many current GCMs, due to the long time integrations and multiple ensembles that are needed for climate studies.

S2 Global-mean aerosol simulation

Table S1 shows global-mean column burdens for the aerosol species treated by the model, for both 1850 and 2000. Also shown are reference ranges for the year 2000, based on one or more studies that have reviewed a range of models. The most notable feature of Table S1 is that the Mk3.6 column burdens of sulfate, OA and dust in 2000 are close to the top of their reference ranges.

Table S1. Comparison of global-mean dry aerosol column burden (in $\rm mg\,m^{-2}$) from the years 1850 and 2000 of the HIST ensemble with a modern-day reference range from other models.

	CSIRO-Mk3.6 1850	CSIRO-Mk3.6 2000	Reference range 2000
Sulfate	2.7	6.0	1.2–6.3[a]
OA	5.2	6.8	0.9–6.7[b]
BC	0.24	0.57	0.09–1.0[c]
Dust	69.9	71.0	16–71[d]
Sea salt	12.8	12.8	4.8–25.8[e]

[a] Liu et al. (2005); Kinne et al. (2006), [b] Kinne et al. (2006); Jathar et al. (2011), [c] Kinne et al. (2006), [d] Zender et al. (2004); Kinne et al. (2006), [e] Kinne et al. (2006).

A contributing factor to the relatively large sulfate burden in the year 2000 is the relatively large emission of DMS ($27\,\rm Tg\,S\,yr^{-1}$), but this also tends to increase the sulfate burden in 1850. The difference in the sulfate burden between 2000 and 1850 is $3.3\,\rm mg\,m^{-2}$. This can be compared with Schulz et al. (2006), who found an average increase since preindustrial times of $2.12\,\rm mg\,m^{-2}$ in the AeroCom models (with a standard deviation of $0.82\,\rm mg\,m^{-2}$) and an average

increase in other studies of 2.70 mg m^{-2} (with a standard deviation of 1.09 mg m^{-2}).

The large OA burden for year-2000 is consistent with our large emissions of OA, in which both the anthropogenic emissions and natural SOA emissions were increased with respect to their default values. However, the relative change in OA burden from 1850 to 2000 is smaller than that obtained for sulfate and BC; this is due to the substantial contribution from SOA (which is unchanged between 1850 and 2000) and the relatively small difference between preindustrial and modern-day biomass-burning emissions in the inventory from Lamarque et al. (2010).

Although we also scaled-up the BC emissions, our global-mean BC column burden for 2000 is not especially large with respect to the reference range. This may reflect the fact that our BC emissions of 9.7 Tg yr^{-1} are still smaller than those assumed in some earlier studies, e.g. an average of 11.9 Tg yr^{-1} for the AeroCom models (Textor et al., 2006).

As mentioned above, the relatively large dust burden can be attributed to the strong effect of the sub-grid gustiness parameterization in the dust uplift scheme (Rotstayn et al., 2011). The sea-salt burden is close to the middle of the range of results from the AeroCom models.

In summary, the total modern-day aerosol burden in CSIRO-Mk3.6 is relatively large, but this is partly related to large emissions of natural aerosols (dust, SOA and sulfate derived from DMS) and a relatively small difference between preindustrial and modern-day biomass-burning emissions in the CMIP5 emission inventory. As discussed above for sulfate, the change between the preindustrial and modern-day burden is larger than average, but not outside the range of earlier studies.

The global-mean aerosol optical depth at 550 nm for the year-2000 simulation is 0.175. Consistent with the relatively large burdens of sulfate, OA and dust, this is somewhat higher than the global average suggested by a composite of satellite retrievals (∼0.15) and by surface-based remote sensing (∼0.135) (Kinne et al., 2006). Similarly, Remer et al. (2008) inferred a global-mean aerosol optical depth of 0.13 to 0.14 over oceans, and 0.19 over land from the Collection 5 Moderate Resolution Imaging Spectroradiometer (MODIS) aerosol products. Our global-mean aerosol optical depth at 550 nm in 1850 is 0.125, so the anthropogenic component (estimated as 2000 minus 1850) is 0.050. This is somewhat larger than an average of 0.029 in the AeroCom models, and an average of 0.041 found in other studies by Schulz et al. (2006). However, it is not outside the range obtained from these studies: the standard deviation was 0.010 for the AeroCom models, and 0.012 for the other models.

S3 Aerosol direct and indirect forcing

It is interesting to consider the breakdown of aerosol forcing into direct and indirect effects. We calculated the direct and first indirect (cloud-albedo) effects as instantaneous forcings, using two pairs of five-year runs with prescribed SSTs and sea ice (similar to the approach used to calculate the RFP in the main text). However, instead of taking the change in net TOA radiation, instantaneous forcings were calculated using double calls to the shortwave radiation scheme, in the manner of Lohmann et al. (2010).

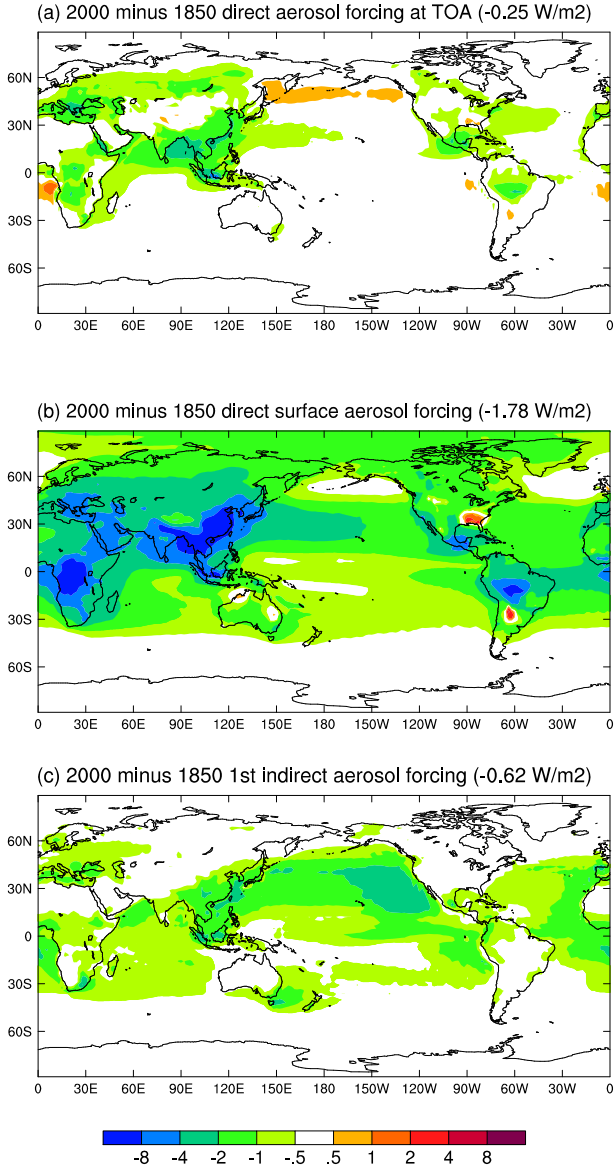

Fig. S1. Anthropogenic aerosol instantaneous forcing (calculated as the difference between 2000 and 1850) in W m^{-2}: **(a)** direct effect at TOA, **(b)** direct effect at the surface, **(c)** first indirect effect at the TOA. The global-mean value for each plot is shown in its header.

Figure S1a shows the direct aerosol forcing at the top of the atmosphere. The global-mean direct TOA forcing (−0.25 W m^{-2}) is close to the best estimate of −0.30 W m^{-2}

from Myhre (2009), who demonstrated consistency between a model and satellite-retrieved values. As expected in the presence of absorbing aerosols, the direct surface forcing in Fig. S1b is generally larger in magnitude than the TOA forcing; the difference ($1.53\,\mathrm{W\,m^{-2}}$ in the global mean) represents atmospheric aerosol absorption. Some areas where the surface forcing is positive (e.g. over the south-eastern USA) occur because biomass-burning aerosol emissions in the inventory of Lamarque et al. (2010) are higher there in 1850 than in 2000. The pattern of the first indirect effect (Fig. S1c) shows some similarity to the direct effect, but there is a noticeable enhancement in regions of persistent low cloud cover, such as the eastern subtropics of the Pacific and Atlantic Ocean basins.

References

Bond, T. C., Streets, D. G., Yarber, K. F., Nelson, S. M., Woo, J., and Klimont, Z.: A technology-based global inventory of black and organic carbon emissions from combustion, J. Geophys. Res., 109, D14 203, doi:10.1029/2003JD003697, 2004.

Cakmur, R. V., Miller, R. L., Perlwitz, J., Geogdzhayev, I. V., Ginoux, P., Koch, D., Kohfeld, K. E., Tegen, I., and Zender, C. S.: Constraining the magnitude of the global dust cycle by minimizing the difference between a model and observations, J. Geophys. Res., 111, D6207, doi:10.1029/2005JD005791, 2006.

Chou, M.-D. and Lee, K.-T.: A Parameterization of the Effective Layer Emission for Infrared Radiation Calculations, J. Atmos. Sci., 62, 531–541, 2005.

Cooke, W. F., Liousse, C., Cachier, H., and Feichter, J.: Construction of a $1^\circ \times 1^\circ$ fossil fuel emission data set for carbonaceous aerosol and implementation and radiative impact in the ECHAM4 model, J. Geophys. Res., 104, 22,137–22,162, 1999.

Dentener, F., Kinne, S., Bond, T., Boucher, O., Cofala, J., Generoso, S., Ginoux, P., Gong, S., Hoelzemann, J. J., Ito, A., Marelli, L., Penner, J. E., Putaud, J.-P., Textor, C., Schulz, M., van der Werf, G. R., and Wilson, J.: Emissions of primary aerosol and precursor gases in the years 2000 and 1750 prescribed datasets for AeroCom, Atmos. Chem. Phys., 6, 4321–4344, doi:10.5194/acp-6-4321-2006, http://www.atmos-chem-phys.net/6/4321/2006/, 2006.

Feichter, J., Kjellström, E., Rodhe, H., Dentener, F., Lelieveld, J., and Roelofs, G.-J.: Simulation of the tropospheric sulfur cycle in a global climate model, Atmos. Environ., 30, 1693–1707, 1996.

Ginoux, P., Chin, M., Tegen, I., Prospero, J. M., Holben, B., Dubovik, O., and Lin, S.-J.: Sources and distributions of dust aerosols simulated with the GOCART model, J. Geophys. Res., 106, 20,255–20,273, doi:10.1029/2000JD000053, 2001.

Ginoux, P., Prospero, J. M., Torres, O., and Chin, M.: Long-term simulation of global dust distribution with the GOCART model: correlation with North Atlantic Oscillation, Environmental Modelling and Software, 19, 113–128, 2004.

Goldstein, A. H. and Galbally, I. E.: Known and unexplored organic constituents in the earth's atmosphere, Environ. Sci. Technol., 41, 1514–1521, 2007.

Gordon, H. B.: A Flux Formulation of the Spectral Atmospheric Equations Suitable for Use in Long Term Climate Modeling, Mon. Weather Rev., 109, 56–64, 1981.

Gordon, H. B., Rotstayn, L. D., McGregor, J. L., Dix, M. R., Kowalczyk, E. A., O'Farrell, S. P., Waterman, L. J., Hirst, A. C., Wilson, S. G., Collier, M. A., Watterson, I. G., and Elliott, T. I.: The CSIRO Mk3 Climate System Model, Technical Paper No. 60, CSIRO Atmospheric Research, Aspendale, Vic., Australia, 134 pp. Available online at http://www.cmar.csiro.au/e-print/open/gordon_2002a.pdf, 2002.

Gordon, H. B., O'Farrell, S. P., Collier, M. A., Dix, M. R., Rotstayn, L. D., Kowalczyk, E. A., Hirst, A. C., and Watterson, I. G.: The CSIRO Mk3.5 Climate Model, Technical Report No. 21, The Centre for Australian Weather and Climate Research, Aspendale, Vic., Australia, 62 pp. Available online at http://www.cawcr.gov.au/publications/technicalreports.php, 2010.

Grant, K. E. and Grossman, A. S.: Description of a Solar Radiative Transfer Model for Use in LLNL Climate and Atmospheric Chemistry Studies, UCRL-ID- 129949, Lawrence Livermore National Laboratory, Livermore, CA, USA, http://www.llnl.gov/tid/lof/documents/pdf/233048.pdf, 17 pp., 1998.

Grant, K. E., Chuang, C. C., Grossman, A. S., and Penner, J. E.: Modeling the spectral optical properties of ammonium sulfate and biomass burning aerosols: parameterization of relative humidity effects and model results, Atmos. Environ., 33, 2603–2620, 1999.

Gregory, D.: The representation of moist convection in atmospheric models, Climate Research Technical Note 54, Hadley Centre, 1995.

Gregory, D. and Rowntree, P. R.: A mass flux convection scheme with representation of cloud ensemble characteristics and stability-dependent closure, Mon. Weather Rev., 118, 1483–1506, 1990.

Guenther, A., Hewitt, C. N., Erickson, D., Fall, R., Geron, C., Graedel, T., Harley, P., Klinger, L., Lerdau, M., McKay, W. A., Pierce, T., Scholes, B., Steinbrecher, R., Tallamraju, R., Taylor, J., and Zimmerman, P.: A global model of natural volatile organic compound emissions, J. Geophys. Res., 100, 8873–8892, 1995.

Holtslag, A. A. M. and Boville, B. A.: Local versus non-local boundary layer diffusion in a global climate model, J. Climate, 6, 1825–1842, 1993.

Jathar, S. H., Farina, S. C., Robinson, A. L., and Adams, P. J.: The influence of semi-volatile and reactive primary emissions on the abundance and properties of global organic aerosol, Atmos. Chem. Phys., 11, 7727–7746, doi:10.5194/acp-11-7727-2011, http://www.atmos-chem-phys.net/11/7727/2011/, 2011.

Jones, A., Roberts, D. L., and Slingo, A.: A climate model study of indirect radiative forcing by anthropogenic sulphate aerosols, Nature, 370, 450–453, 1994.

Kanakidou, M., Seinfeld, J. H., Pandis, S. N., Barnes, I., Dentener, F. J., Facchini, M. C., Dingenen, R. V., Ervens, B., Nenes, A., Nielsen, C. J., Swietlicki, E., Putaud, J. P., Balkanski, Y., Fuzzi, S., Horth, J., Moortgat, G. K., Winterhalter, R., Myhre, C. E. L., Tsigaridis, K., Vignati, E., Stephanou, E. G., and Wilson, J.: Organic aerosol and global climate modelling: a review, Atmos. Chem. Phys., 5, 1053–1123, 2005.

Kettle, A. J. and Andreae, M. O.: Flux of dimethylsulfide from the oceans: A comparison of updated data sets and flux models, J. Geophys. Res., 105, 26,793–26,808, 2000.

Kettle, A. J., Andreae, M. O., Amouroux, D., Andreae, T. W., Bates, T. S., Berresheim, H., Bingemer, H., Boniforti, R., Curran, M. A. J., DiTullio, G. R., Helas, G., Jones, G. B., Keller, M. D., Kiene, R. P., Leck, C., Levasseur, M., Malin, G., Maspero, M., Matrai, P., McTaggart, A. R., Mihalopoulos, N., Nguyen, B. C., Novo, A., Putaud, J. P., Rapsomanikis, S., Roberts, G., Schebeske, G., Sharma, S., Simo, R., Staubes, R., Turner, S., and Uher, G.: A global database of sea surface dimethylsulfide (DMS) measurements and a procedure to predict sea surface DMS as a function of latitude, longitude and month, Global Biogeochem. Cycles, 13, 399–444, 1999.

Kinne, S., Schulz, M., Textor, C., Guibert, S., Balkanski, Y., Bauer, S. E., Berntsen, T., Berglen, T. F., Boucher, O., Chin, M., Collins, W., Dentener, F., Diehl, T., Easter, R., Feichter, J., Fillmore, D., Ghan, S., Ginoux, P., Gong, S., Grini, A., Hendricks, J., Herzog, M., Horowitz, L., Isaksen, I., Iversen, T., Kirkevåg, A., Kloster, S., Koch, D., Kristjansson, J. E., Krol, M., Lauer, A., Lamarque, J. F., Lesins, G., Liu, X., Lohmann, U., Montanaro, V., Myhre, G., Penner, J., Pitari, G., Reddy, S., Seland, O., Stier, P., Takemura, T., and Tie, X.: An AeroCom initial assessment – optical properties in aerosol component modules of global models, Atmos. Chem. Phys., 6, 1815–1834, 2006.

Kraus, E. B. and Turner, J.: A one dimensional model of the seasonal thermocline II. The general theory and its consequences., Tellus, 19, 98–106, 1967.

Lamarque, J.-F., Bond, T. C., Eyring, V., Granier, C., Heil, A., Klimont, Z., Lee, D., Liousse, C., Mieville, A., Owen, B., Schultz, M. G., Shindell, D., Smith, S. J., Stehfest, E., Van Aardenne, J., Cooper, O. R., Kainuma, M., Mahowald, N., McConnell, J. R., Naik, V., Riahi, K., and van Vuuren, D. P.: Historical (1850–2000) gridded anthropogenic and biomass burning emissions of reactive gases and aerosols: methodology and application, Atmos. Chem. Phys., 10, 7017–7039, doi:10.5194/acp-10-7017-2010, 2010.

Lana, A., Bell, T. G., Simó, R., Vallina, S. M., Ballabrera-Poy, J., Kettle, A. J., Dachs, J., Bopp, L., Saltzman, E. S., Stefels, J., Johnson, J. E., and Liss, P. S.: An updated climatology of surface dimethlysulfide concentrations and emission fluxes in the global ocean, Glob. Biogeochem. Cyc., 25, GB1004, doi:10.1029/2010GB003850, 2011.

Lee, S., Kim, H. K., Yan, B., Cobb, C. E., Hennigan, C., Nichols, S., Chamber, M., Edgerton, E. S., Jansen, J. J., Hu, Y., Zheng, M., Weber, R. J., and Russell, A. G.: Diagnosis of Aged Prescribed Burning Plumes Impacting an Urban Area, Environ. Sci. Technol., 42, 1438–1444, doi:10.1021/es7023059, 2008.

Liss, P. S. and Merlivat, L.: Air-sea gas exchange rates: Introduction and synthesis, in: The role of air-sea gas exchange in geochemical cycling, edited by Menard, P. B., pp. 113–127, D. Reidel, Norwell, Mass., 1986.

Liu, X., Penner, J. E., and Herzog, M.: Global modeling of aerosol dynamics: Model description, evaluation, and interactions between sulfate and nonsulfate aerosols, J. Geophys. Res., 110, D18 206, doi:doi:10.1029/2004JD005674, 2005.

Lohmann, U., Feichter, J., Chuang, C. C., and Penner, J. E.: Prediction of the number of cloud droplets in the ECHAM GCM, J. Geophys. Res., 104, 9169–9198, 1999.

Lohmann, U., Rotstayn, L., Storelvmo, T., Jones, A., Menon, S., Quaas, J., Ekman, A. M. L., Koch, D., and Ruedy, R.: Total aerosol effect: radiative forcing or radiative flux perturbation?, Atmos. Chem. Phys., 10, 3235–3246, 2010.

Louis, J.-F.: A Parametric Model of Vertical Eddy Fluxes in the Atmosphere, Bound. Layer Meteorol., 17, 187–202, 1979.

McGregor, J. L.: Economical Determination of Departure Points for Semi-Lagrangian Models, Mon. Weather Rev., 121, 221–230, 1993.

Myhre, G.: Consistency Between Satellite-Derived and Modeled Estimates of the Direct Aerosol Effect, Science, 325, 187–190, doi:10.1126/science.1174461, 2009.

Nightingale, P. D., Malin, G., Law, C. S., Watson, A. J., Liss, P. S., Liddicoat, M. I., Boutin, J., and Upstill-Goddard, R. C.: In situ evaluation of air-sea gas exchange parameterizations using novel conservative and volatile tracers, Global Biogeochem. Cycles, 14, 373–387, 2000.

O'Dowd, C. D., Smith, M. H., Consterdine, I. E., and Lowe, J. A.: Marine aerosol, sea-salt, and the marine sulphur cycle: a short review, Atmos. Environ., 31, 73–80, 1997.

O'Farrell, S. P.: Investigation of the dynamic sea ice component of a coupled atmosphere-sea ice general circulation model, J. Geophys. Res., 103, 15 751–15 782, 1998.

Pacanowski, R. C.: MOM 2 Version 2, Documentation, User's Guide and Reference Manual, GFDL Ocean Technical Report 3.2, Geophysical Fluid Dynamics Laboratory/NOAA, Princeton, NJ, USA, http://www.gfdl.noaa.gov/cms-filesystem-action?file=model_development/ocean/manual2.2.pdf, 1996.

Penner, J. E., Chuang, C. C., and Grant, K.: Climate forcing by carbonaceous and sulfate aerosols, Climate Dyn., 14, 839–851, 1998.

Prospero, J. M., Ginoux, P., Torres, O., Nicholson, S. E., and Gill, T. E.: Environmental characterization of global sources of atmospheric soil dust identified with the NIMBUS 7 Total Ozone Mapping Spectrometer (TOMS) absorbing aerosol product, Rev. Geophys., 40, 1002, doi:10.1029/2000RG000095, 2002.

Pye, H. O. T., Chan, A. W. H., Barkley, M. P., and Seinfeld, J. H.: Global modeling of organic aerosol: the importance of reactive nitrogen (NO_x and NO_3), Atmos. Chem. Phys., 10, 11 261–11 276, doi:10.5194/acp-10-11261-2010, http://www.atmos-chem-phys.net/10/11261/2010/, 2010.

Remer, L. A., Kleidman, R. G., Levy, R. C., Kaufman, Y. J., Tanre, D., Mattoo, S., Martins, J. V., Ichoku, C., Koren, I., Yu, H., and Holben, B. N.: Global aerosol climatology from the MODIS satellite sensors, J. Geophys. Res., 113, D14S07, doi:10.1029/2007JD009661, 2008.

Rotstayn, L. D.: A physically based scheme for the treatment of stratiform clouds and precipitation in large-scale models. I: Description and evaluation of the microphysical processes, Q. J. R. Meteorol. Soc., 123, 1227–1282, 1997.

Rotstayn, L. D.: A physically based scheme for the treatment of stratiform clouds and precipitation in large-scale models. II: Comparison of modelled and observed climatological fields, Q. J. R. Meteorol. Soc., 124, 389–415, 1998.

Rotstayn, L. D.: On the "tuning" of autoconversion parameterizations in climate models, J. Geophys. Res., 105, 15,495–15,507, 2000.

Rotstayn, L. D. and Liu, Y.: A smaller global estimate of the second indirect aerosol effect, Geophys. Res. Lett., 32, L05708, doi:10.1029/2004GL021922, 2005.

Rotstayn, L. D. and Liu, Y.: Cloud droplet spectral dispersion and the indirect aerosol effect: Comparison of two treatments

in a GCM, Geophys. Res. Lett., 36, L10801, doi:10.1029/2009GL038216, 2009.

Rotstayn, L. D. and Lohmann, U.: Simulation of the tropospheric sulfur cycle in a global model with a physically based cloud scheme, J. Geophys. Res., 107, 4592, doi:10.1029/2002JD002128, 2002.

Rotstayn, L. D., Ryan, B. F., and Katzfey, J. J.: A scheme for calculation of the liquid fraction in mixed-phase stratiform clouds in large-scale models, Mon. Weather Rev., 128, 1070–1088, 2000.

Rotstayn, L. D., Cai, W., Dix, M. R., Farquhar, G. D., Feng, Y., Ginoux, P., Herzog, M., Ito, A., Penner, J. E., Roderick, M. L., and Wang, M.: Have Australian Rainfall and Cloudiness Increased Due to the Remote Effects of Asian Anthropogenic Aerosols?, J. Geophys. Res., 112, D09202, doi:10.1029/2006JD007712, 2007.

Rotstayn, L. D., Collier, M. A., Feng, Y., Gordon, H. B., O'Farrell, S. P., Smith, I. N., and Syktus, J.: Improved simulation of Australian climate and ENSO-related rainfall variability in a GCM with an interactive aerosol treatment, Int. J. Climatol., 30, 1067–1088, doi:10.1002/joc.1952, 2010.

Rotstayn, L. D., Collier, M. A., Mitchell, R. M., Qin, Y., Campbell, S. K., and Dravitzki, S. M.: Simulated enhancement of ENSO-related rainfall variability due to Australian dust, Atmos. Chem. Phys., 11, 6575–6592, doi:10.5194/acp-11-6575-2011, http://www.atmos-chem-phys.net/11/6575/2011/, 2011.

Schulz, M., Textor, C., Kinne, S., Balkanski, Y., Bauer, S., Berntsen, T., Berglen, T., Boucher, O., Dentener, F., Guibert, S., Isaksen, I. S. A., Iversen, T., Koch, D., Kirkevåg, A., Liu, X., Montanaro, V., Myhre, G., Penner, J. E., Pitari, G., Reddy, S., Seland, Ø., Stier, P., and Takemura, T.: Radiative forcing by aerosols as derived from the AeroCom present-day and preindustrial simulations, Atmos. Chem. Phys., 6, 5225–5246, doi:10.5194/acp-6-5225-2006, http://www.atmos-chem-phys.net/6/5225/2006/, 2006.

Textor, C., Schulz, M., Guibert, S., Kinne, S., Balkanski, Y., Bauer, S., Berntsen, T., Berglen, T., Boucher, O., Chin, M., Dentener, F., Diehl, T., Easter, R., Feichter, H., Fillmore, D., Ghan, S., Ginoux, P., Gong, S., Grini, A., Hendricks, J., Horowitz, L., Huang, P., Isaksen, I., Iversen, T., Kloster, S., Koch, D., Kirkevåg, A., Kristjansson, J. E., Krol, M., Lauer, A., Lamarque, J. F., Liu, X., Montanaro, V., Myhre, G., Penner, J., Pitari, G., Reddy, S., Seland, Ø., Stier, P., Takemura, T., and Tie, X.: Analysis and quantification of the diversities of aerosol life cycles within AeroCom, Atmos. Chem. Phys., 6, 1777–1813, 2006.

Van Leer, B.: Towards the Ultimate Conservative Difference Scheme. V. A New Approach to Numerical Convection, J. Comp. Phys., 23, 276–299, 1977.

Visbeck, M., Marshall, J., Haine, T., and Spall, M.: Specification of eddy transfer coefficients in coarse-resolution ocean circulation models, J. Phys. Oceanogr., 27, 381–402, doi:10.1175/1520-0485(1997)027⟨0381:SOETCI⟩2.0.CO;2, 1997.

Zender, C. S., Miller, R. L., and Tegen, I.: Quantifying mineral dust mass budgets: terminology, constraints, and current estimates, Eos, 85, 509–512, doi:10.1029/2004EO480002, 2004.